Comparing 545 Million Years of Sea-Level Change: New Insights from the TopoChronia QGIS Plugin

Florian Franziskakis[1], Christian Vérard[2], Sébastien Castelltort[2], Grégory Giuliani[1]

[1]Institute for Environmental Sciences, University of Geneva, Boulevard Carl-Vogt 66, 1205 Geneva, Switzerland
(florian.franziskakis,gregory.giuliuani)@unige.ch
[2]Department of Earth Sciences, University of Geneva, Rue des Maraîchers 13, 1205 Geneva, Switzerland
(christian.verard, sebastien.castelltort)@unige.ch

Keywords: Tectonics, Sea-Level, Climate, Palaeogeography, PANALESIS.

Abstract

Palaeogeography is the study of the geography in the geological past, focusing on reconstructing the position of continents, oceans and mountain ranges over millions of years, helping scientists to understand past climates, the evolution of life and quantify sea-level variations. Plate tectonic models are essential for reconstructing palaeogeography, as they provide information about the position and age of geological features controlling the topography. The PANALESIS model, for instance, can be used to create fully quantified palaeogeographic reconstructions and sea-level variations estimates. However, the data and code used to produce previous results using PANALESIS were never published, were dependent on proprietary software, and can no longer be run due to software obsolescence, making them impossible to reproduce. To address this, we have entirely rewritten and enhanced the source code into a QGIS plugin named `TopoChronia`. In this paper, we present sea-level curves derived from the new palaeogeographic maps over the Phanerozoic, and compare them with the original PANALESIS sea-level curve as well as other data obtained with sequential stratigraphic studies. We discuss possible causes explaining differences in results. The `TopoChronia` plugin is available at https://github.com/florianfranz/topo_chronia

1. Introduction

Over the Phanerozoic, many studies have provided reconstructions of sea-level fluctuations at the global scale (eustasy). Understanding these variations is useful in many disciplines of the geosciences, including palaeoclimatology (Goddéris et al., 2014; Lunt et al., 2016).

One one hand, sequence stratigraphy, the study of rock strata relationship and patterns linked to sea-level variations, has long been used to understand global and local changes throughout the Phanerozoic starting with Vail et al. (1977); Payton (1977); Vail et al. (1991) and Miall (1996). Their methodology laid the foundation for the creation of several curves (Haq et al., 1987; Wilgus et al., 1988; Hallam and Cohen, 1997; Miller et al., 2005; Haq and Al-Qahtani, 2005; Haq and Schutter, 2008; Haq, 2018). Snedden and Liu (2010) also provided a curve derived (and rescaled) from Haq et al. (1987); Hardenbol et al. (1998) and Haq and Schutter (2008).

These studies showed two peaks reaching above +200m in the Late Cretaceous and in the mid-Palæozoic; compared to our present-day sea-level reference (set at 0m). More recently, Vérard (2024) generated a composite curve from the curves of Haq et al. (1987); Haq and Al-Qahtani (2005); Haq and Schutter (2008) and Haq (2018), rescaled to one of the most recent chronostratigraphic chart; This composite curve is referred herein to as the "Haq's curves".

On the other hand, the plate tectonic theory, defined mainly by McKenzie and Parker (1967); Morgan (1968); Le Pichon (1968); Isacks et al. (1968) and Vine and Hess (1968), paved the way for the development of plate tectonic models.

These models showed that the global ocean basin size changed through time, influenced by the movement of plates, and the distribution of continents, as discussed for instance in Wright et al. (2020). Plate tectonics models have been used to evaluate sea-level change curves over the Phanerozoic and show similar trend as curves derived from stratigraphy (Vérard et al., 2015; Marcilly et al., 2022), despite large uncertainties.

These uncertainties mainly arise from how sea-level curves are derived from the plate tectonics models. Some models create semi-quantitative palaeogeographic maps with elevation ranges (Scotese, 2021), while other models, like PANALESIS (Vérard, 2019) are capable of producing fully quantified palaeotopographic maps, from which global sea-level may be derived, and accounted for, into palaeogeographic maps.

PANALESIS is a plate tectonic model covering 100% of the Earth's surface with 44 distinct reconstructions over the Phanerozoic for what concerns PANALESIS v0 (Vérard, 2019). The model uses a dual-control approach, which means that it is (i) based on present-day geological evidence moved to their past location and (ii) one reconstruction has to be dynamically coherent with the one preceding it and controls the next one.

The steps to generate these fully quantified maps were described previously in Vérard et al. (2015) which used the UNIL model (Stampfli and Borel, 2002; Stampfli et al., 2013). The code was however never released and both data the software used to process it were proprietary.

With the aim of putting the FAIR (Findable, Accessible, Interoperable, Reusable) principles into practice, for both data and software (Wilkinson et al., 2016; Barker et al., 2022), we have entirely re-written the code into a QGIS plugin called `TopoChronia`, available on GitHub at https://github.com/florianfranz/topo_chronia.

In this paper, we compare the sea-level curve obtained using `TopoChronia` for the entire Phanerozoic (back to the 545 Million year (Ma) reconstruction) with the original curve from Vérard et al. (2015). We also compare our results with Haq's curves. We finally discuss issues related to reference data, water load correction, input model version management and interpolation method.

2. Methodology

We use the PANALESIS model features polylines describing geological settings and associated environments. From the original lines, we create points to which we assign a typical elevation value, based on the study of present-day Earth's topography of these geological settings (Vérard, 2017). This results in a synthetic topography. Contrary to other attempts which rely on moving the present-day topography to its past location, as for instance with the TerraAntiqua QGIS plugin (Aminov et al., 2023), the topography generated by `TopoChronia` is fully and exclusively derived from features encompassed in the plate tectonic model.

We first define oceans, using mid-oceanic ridges and isochrons (lines marking rocks of the same age on the ocean floor) vertices, and define their elevation value which is controlled by the feature age, according to plate cooling model equations. While Stein and Stein (1992) arbitrarily employed two models (a half-space model proportional to the square root of the age, and a plate cooling model with an exponential age dependency), Vérard (2017) demonstrated that a single plate cooling model, characterized by a combination of constants and an exponential decay term, more accurately represents the complete seafloor bathymetry when corrected for sediment loading. Sediment thickness is therefore accounted for separately.

Second, we generate other plate boundaries settings, such as active margins and collision zones. We also define intra-plate areas like passive margins, areas affected by rifting, and abandoned arcs. For each vertex of input line features, we create a perpendicular profile with varying length depending on the feature type. Each vertex of the profile is then assigned an elevation, that is controlled by the distance to the original line position and by the age of the feature. One example of a typical collision profile evolution is given in Figure 1.

We then add other geological features such as cratons (large, stable blocks of the Earth's crust that forms the ancient core of a continent), hot-spots, and continents areas not affected by other settings. Finally, we merge and clean the final points layer to avoid different settings profiles crossing each other that would create an incoherent topography.

Once the points are cleaned, we interpolate a global raster with a resolution of approximately 10x10km from these points using the QGIS Triangulated Irregular Network (TIN) method, as it has shown to perform best in these circumstances (Franziskakis et al., in prep). Using the `native:rastersurfacevolume` algorithm in QGIS (QGIS Development Team, 2025), we calculate the volume below the elevation of 0m and compare it with the present-day volume of oceans, calculated with the same algorithm using ETOPO 2022 data (NOAA, 2022).

Assuming a constant oceanic volume through time, we can therefore estimate the increase or decrease in sea-level required to match this volume, using Airy equations for eustasy (Allen and Allen, 2005). The sea-level change (rise or fall) is dependent on the density difference between oceanic water and the basement rocks. It can be expressed as:

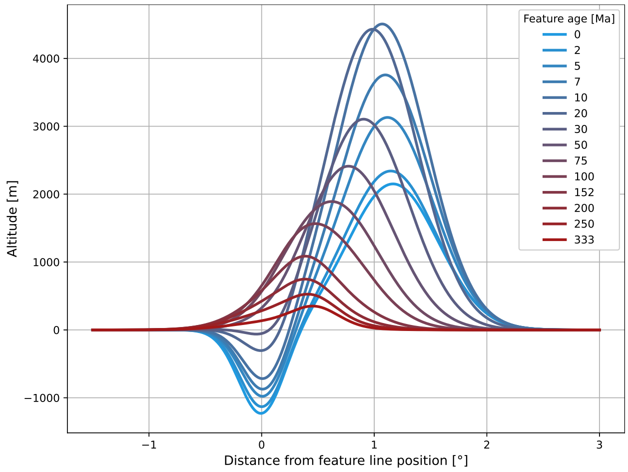

Figure 1. Example of synthetic elevation associated with a collision zone, evolving alongside a profile that is perpendicular to the original collision line. Elevation is controlled by the feature age and by the distance from the original feature line.

$$\Delta_{SL} = \left(\frac{\rho_m - \rho_w}{\rho_m}\right)(h_2 - h_1) \tag{1}$$

where:

Δ_{SL} is the sea-level change [m],
ρ_m is the density of the basement (3300 [kg/m^3]),
ρ_w is the density of water (1027 [kg/m^3]),
$h_2 - h_1$ represents the change in water column height [m].

For any added water height $h = h_2 - h_1$, the sea-level rise accounted for subsidence, and the subsidence (S) itself can therefore be expressed as:

$$\Delta_{SL} \approx 0.69 \cdot h, \quad S \approx 0.31 \cdot h \tag{2}$$

Applied to palaeogeographic reconstructions, this implies modifying the elevation value to every pixel of the map by first subtracting the ΔSL everywhere, to define the new sea-level. Second, we also correct for subsidence (sinking of the oceanic crust) caused by the addition of water. This correction is applied to all pixels below water.

For pixels that are located in-between the original sea-level and the ΔSL value, we apply a partial correction corresponding to only the added water column corresponding to the difference of elevation between the initial elevation and ΔSL. We finally correct the subsidence accordingly.

We compare the PANALESIS v0 results (spanning from 545 Ma to present-day), and include the PANALESIS v1 (still under development) from Vérard (2021) results from 340 to 540 Ma, as the two versions (v0 & v1) and the Haq-curves are only comparable on the 330 to 540 time range.

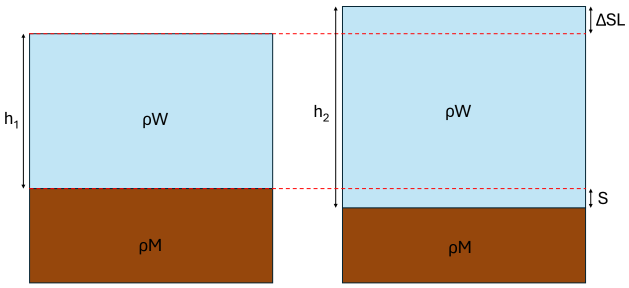

Figure 2. Water load correction according to Airy's model, modified after Allen and Allen (2005). The added water column is divided into an extra height of water above initial level (ΔSL) and subsidence of the oceanic floor (S).

3. Results

We compare our results with previously published data from plate tectonic models, and compare them against sequential stratigraphy results (Haq's curves). Our results, including maps and sea-level summaries are available on Zenodo (https://doi.org/10.5281/zenodo.15396265).

3.1 Comparison with original curves

3.1.1 Uncorrected Sea-Level We refer as "uncorrected sea-level", the total required added water height (h in Equation 2) to reach the full reference volume. This represents the absolute amount of water we need to pour into the oceans before any correction on topography for ΔSL and subsidence.

The original and new uncorrected sea-level curves (Figure 3) tend to follow the same trend, oscillating between lows (at approximately 0, 180, 330 and 420 Ma) and highs (at ca. 100, 240, 380, and beyond 460 Ma).

Some discrepancies are however observed with large differences, for instance around 165, 250, 420 and beyond 500 Ma. The median of absolute difference between the original and new uncorrected values is 66.5m, while the mean value is 71.9m. Note that values beyond 500 Ma are considerably high due to the fact that the plate tectonic model does not cover 100% of the Earth surface. Excluding values older than 500 Ma and after, the median and mean differences become respectively 46.5 and 64.3m.

3.1.2 Corrected Sea-level Given a new water column height to add (uncorrected values), a ΔSL is added, alongside the corresponding subsidence S. We therefore refer to corrected sea-level as the ΔSL part of the added water column, as defined in Equation 2.

We observe in Figure 4 that the new `TopoChronia` corrected sea-level curve from PANALESIS v0 follows the same trend as the uncorrected one, with similar anomalies. The amplitude of variation seems to be higher than the initial curve from 2015, due to a difference in calculating the correction for water load (see Section 4). The median of absolute difference between the original and new corrected values on v0 is 49.6m, while the mean value is 59.8m. Excluding values at 500 Ma and after, the median and mean differences become respectively 47.2 and 50.5m.

We observe a completely different trend between the v0 and v1 curves beyond 500 Ma, with decreasing sea-level for the v1.

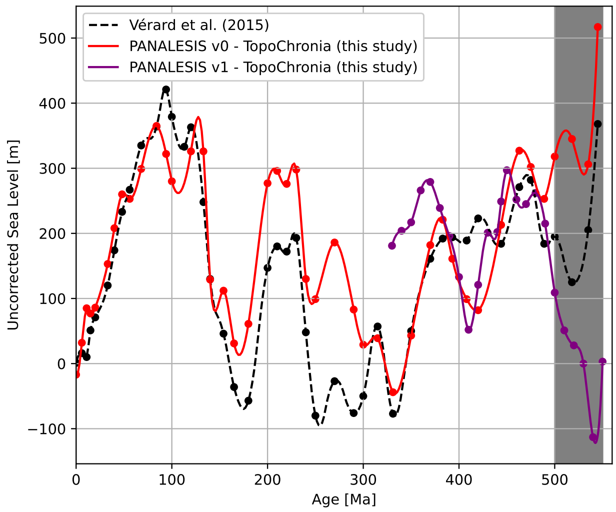

Figure 3. Uncorrected sea-level [m] using PANALESIS v0 and v1 for the Phanerozoic. In black, original results Vérard et al. (2015), in red and purple, new results using `TopoChronia` on PANALESIS v0 and v1, respectively. Dark grey area indicates time ranges for which the PANALESIS v0 and UNIL model do not cover 100% of the Earth surface, PANALESIS v1, under construction, covers 100% back to 750 Ma.

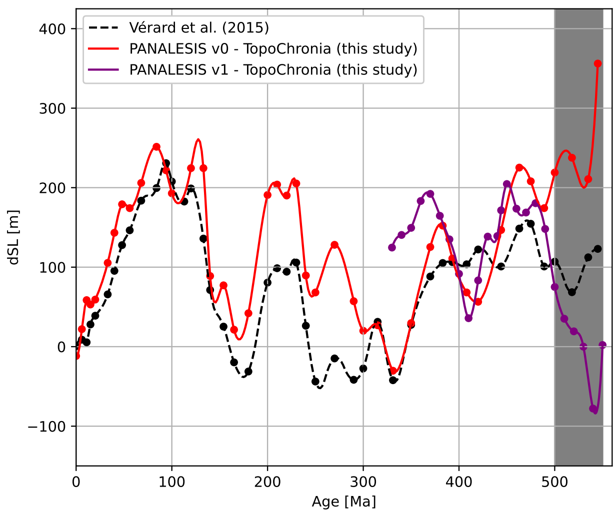

Figure 4. Corrected sea-level [m] performance of PANALESIS v0 and v1 for the Phanerozoic. Same legend as for Figure 3.

This can be explained by the switch of the full Earth coverage by the v1, which extends back in time to ca. 750 Ma (Vérard, 2021). This allows to have more complete reconstructions, and compare where we have data from both versions, i.e. between 330 and 540 Ma.

3.2 Comparison with Haq's curves

Haq's curves from Vérard (2024) have a temporal resolution of 0.1 Ma, which is much shorter than the intervals we have in-between PANALESIS reconstructions, varying from 6 to 24 Ma for v0, and with 10 Ma steps for v1. We calculated the mean Haq's sea-level values for each PANALESIS time interval and compared them with the sea-level obtained using the PANALESIS reconstruction, by calculating their difference.

We then generate the mean, median, maximum and minimum of these differences for the entire series (where data is comparable as highlighted in Figure 4). The statistics are provided in Table 1. Sea-level curves comparison with Haq's curves for Vérard et al. (2015) and PANALESIS v0 are provided in Figure 5, and in Figure 6 for PANALESIS v1.

We observe that our mean differences compared to Haq's curves using `TopoChronia` on PANALESIS v0 is much higher than the original curve from Vérard et al. (2015), with respective values of 60.2 and 47.1m. We discuss possible reasons for these performances in Section 4.

	TopoChronia v0 0 - 500	TopoChronia v1 330 - 540	Vérard et al. 2015 UNIL 0 - 500
Mean	60.1594	42.7190	47.1240
Median	37.7314	27.4410	41.1070
Max	243.5463	111.0964	138.3365
Min	1.3245	3.3149	5.3841

Table 1. Comparison of differences between Haq's curves (Vérard, 2024) versus `TopoChronia` and Vérard et al. (2015)

For what concerns PANALESIS v1 performance, we observe a mean difference of 42.7m with Haq's curves, and an overall better performance for all indicators, including the median of the differences at 27.4m, compared to 41.1m for Vérard et al. (2015).

The v1 curve shows a remarkable fit from 380 Ma until the end of the Phanerozoic. Younger values (form 330 to 370 Ma) systematically show higher values, but are still following the same increasing trend within this time frame.

4. Discussion

Overall, both the original and the new v0 curves seem to follow similar tendencies, but differ for some reconstructions. A few factors may explain these differences, and are discussed below.

4.1 Oceans volumes used for comparison

The reference volume used in this study is based on the ETOPO volume under z = 0m, whereas the 2015 reference volume was the volume of the 000 Ma (present-day) reconstruction (i.e. stemming from the ca. 545 Ma reconstructions), which was significantly higher than ETOPO.

We prefer to compare directly with real-world data as a means to assess the accuracy of the present-day reconstruction. The volume we obtained using the `native:rastersurfacevolume` algorithm on ETOPO data is 1.3366×10^{18} m^3, which is aligning with recent estimates of 1.3324×10^{18} m^3 from Charette and Smith (2010).

For comparison, our present-day reconstruction using PANALESIS v0 yields a volume of 1.3429×10^{18} m^3, only 0.47 % higher than the reference. In terms of relative sea-level, this means a ΔSL of -11.71m.

While this error percentage might seem negligible, this still represents an absolute difference in volume of about 6.6×10^{15} m^3, approximately 1.7× the volume of the Mediterranean Sea, estimated to be 3.84×10^{15} m^3, according to Zonn et al. (2021).

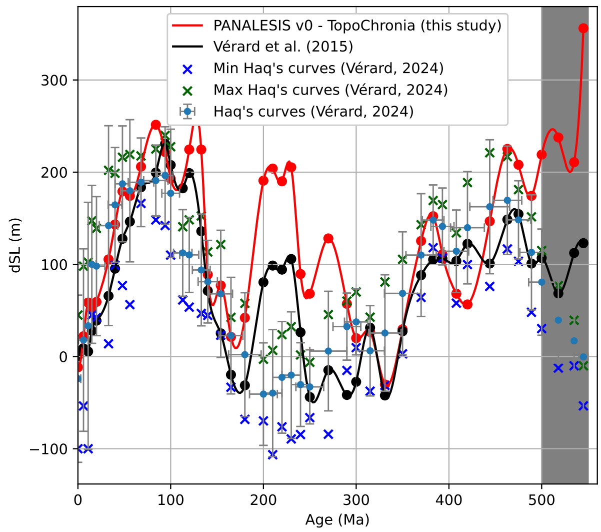

Figure 5. Sea-level (black) from Vérard et al. (2015) and PANALESIS v0 using `TopoChronia` (red) compared to Haq's curves values from Vérard (2024). The data have been resampled to match PANALESIS reconstruction intervals (horizontal error bars). Vertical error bars represent the two sigma errors calculated from all values within each time interval. Green and blue crosses indicate the maximum and minimum values of Haq's curves within each interval.

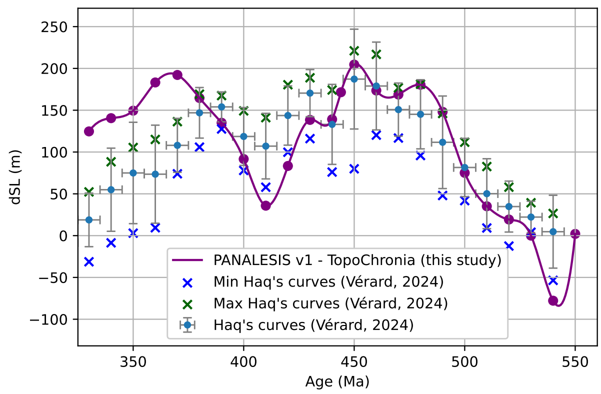

Figure 6. Sea-level (purple) PANALESIS v1 curve using `TopoChronia` compared to Haq's curves values from Vérard (2024). Same legend as in Figure 5.

4.2 Water load correction

In Vérard et al. (2015), a constant ratio of $\Delta SL = 0.55 \times h$ was used, instead of our implementation of Airy's equations (Equation 1) which approximates a higher ratio of $0.69 \times h$ (Equation 2). This leads to a 25% higher ΔSL for the same uncorrected value.

Beyond the change in correcting factor only, our new results differ by the method used to accommodate sea-level change, especially how the reference (0m of elevation) is accounted for. In this study, we opted out for a direct reset of the reference sea-level to be equal to ΔSL, and to also add the subsidence by increasing the seafloor depth, with values being defined in Equation 1.

This leads to a different and more direct approach depicted in Figure 7. With a theoretical 100m of added water height, we first reset the sea-level to ΔSL, in this case, lowering the elevation to all points by 69m. We then correct for the new water load and subsidence of points that are now located below the new sea-level. We apply a partial correction of subsidence for points that were not below water initially but only after adding the 69m of ΔSL, with the fraction of subsidence related to the water added.

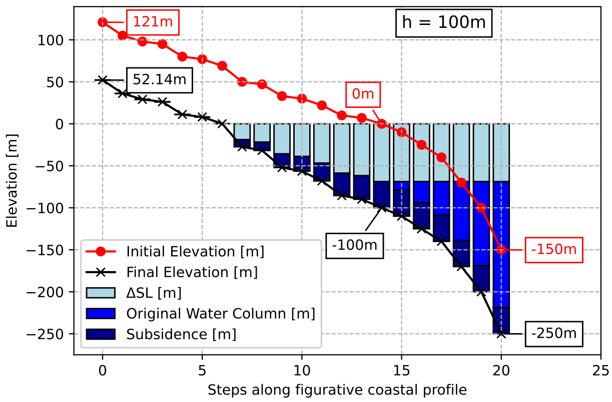

Figure 7. Figurative coastal profile water load correction example, for an added water column height (h) of 100m, ΔSL of $\approx$ 69m (light blue) and subsidence (S) of $\approx$ 31m (dark blue). The original water column (regular blue) corresponds to the initial elevation, and applies only for points originally under water (initial elevation <0m).

4.3 Input data modifications

Divergences between `TopoChronia`-derived and initial results can be further analyzed beyond only the sea-level result, by looking at potential differences in input feature ages, which controls the elevation.

We identified important differences between the UNIL model used in Vérard et al. (2015) and the PANALESIS v0, as illustrated in Figure 8A. This figure shows, for instance that some passive margins ages changed to much younger values (originally 165 to 75 or 90 Ma), heavily affecting topography (Figure 8B), and consequently the oceans volume.

This feature age difference arises from how passive margins are described in each model: for the UNIL model, the age refers to the initial rifting phase leading to the formation of the passive margin, whereas PANALESIS uses the separation of the continental crust age.

4.4 Change in interpolation method

The original maps were obtained using the ArcGIS Natural Neighbour (NatN) method to interpolate the Digital Elevation Model (DEM), as it was convenient, quick, and created good looking maps. At the time, no quantification of errors had however been done to assess whether or not other interpolation methods, such as Kriging, Inverse Distance Weighted (IDW) or Nearest Neighbour (NN) could perform better.

We show in another study (Franziskakis et al, in prep) that the TIN method from QGIS is the best method to interpolate a global topographic raster from a highly irregular grid of nodes.

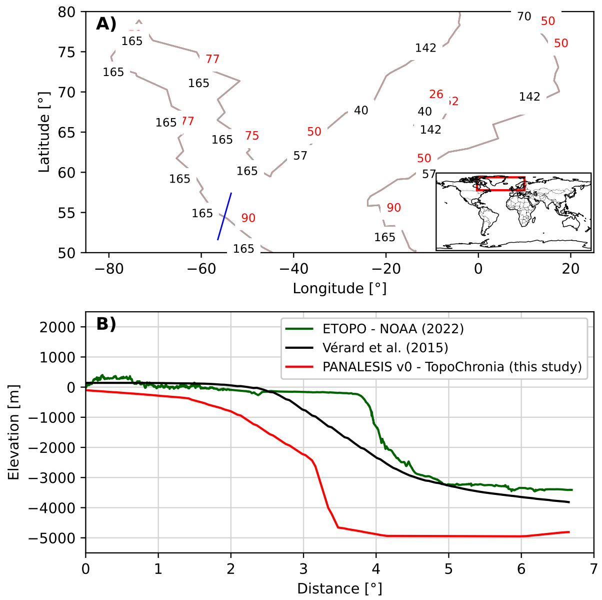

Figure 8. A) Example of discrepancies in feature ages of passive margins from the PANALESIS v0 model present-day reconstruction (grey lines). Values in black are the ages defined in the UNIL model and used in Vérard et al. (2015), while ages in red are ages defined in the PANALESIS v0 model and used for `TopoChronia`. The blue line represents a profile for which we measured the elevation, shown in B).

We have hence chosen this method instead. We calculated the oceans volume for rasters interpolated with the NatN and the TIN methods, and found an uncertainty of about 1%, which represents about 35 meters of sea-level increase for the present-day.

4.5 Uncertainties

The reliability of PANALESIS v0 has already been discussed in Vérard (2022), who showed, for instance, that the synthetic coastline generated by the model matched the actual coastline in 60% of the time for the present-day reconstruction. This can be explained by uncertainties in the original model features position, and the time lapse between reconstructions.

Feature ages uncertainties are critical to consider, as the age is one primary controlling factor of topography in PANALESIS. When dealing with deep-time reconstructions, uncertainties of several million years are frequent, and complex situations (highlighted, for instance in Figure 8), where the age, and therefore the topography of one feature dramatically changes because of a different interpretation.

Note that we doubt that the uncertainty on any feature ages be greater than 10%, but in some rare cases, as per Figure 8, the interpretation of some ages might be higher. To test the sensitivity of the topography to the age of the features, we examined six scenarios on the present-day reconstruction with varying feature ages, increasing or decreasing them by 10%, 25%, and 50%. The results for oceans volume, area and mean depth are provided in Table 2. They depict an extreme sensitivity to differences in feature ages. The scenario with 50% older ages yields an oceanic volume of only 1.2821×10^{18} m^3, which translates in a ΔSL of 105.38m (or an uncorrected water height value of 153m).

	Volume (E+18m^3)	Area (E+14m^2)	ΔSL (m)	Mean Depth (m)
+50%	1.3280	3.4493	+17.22	3812
+25%	1.3398	3.5011	-5.51	3817
+10%	1.3407	3.5121	-7.58	3784
Base	1.3439	3.5248	-13.78	3826
-10%	1.3376	3.5343	-1.38	3742
-25%	1.32665	3.54504	+19.97	3850
-50%	1.2821	3.5257	+105.38	3636

Table 2. Different scenarios for changes in all feature ages of the PANALESIS present-day reconstruction. Comparison of oceanic volume, area, sea-level difference, and mean depth for each scenario.

Looking at the variations of oceanic areas for the different scenarios confirms what we observed in Figure 8, with regards to older passive margin features being responsible for wider continents (and thus smaller oceans). This is however partially balanced by the seafloor depth, which becomes greater with older ages, but with smaller proportions than passive margins.

Concerning sea-level, the fact that reference of the original curve from Vérard et al. (2015) was based on the present-day reconstruction adds uncertainties because it does not inform us about differences between the oceanic volume of this reconstruction and the actual volume.

PANALESIS v1 reconstructions (still under development) were not tested against Haq's curves before this study, and it is encouraging to see a good match that follows long-term trends (up to 100 Ma periods). This supports the assessment by Vérard (2024) that plate tectonics is the main driving factor for long-term evolution of sea-level, with ±60m uncertainties due to shorter-term variations possibly explained by melting of ice caps. Similar estimates have been done to assess the impact of a complete melting of the Greenland and Antarctic ice sheet on the current sea-level, with respectively 7m (Gregory et al., 2004) and 58m (Fretwell et al., 2013).

Even the Haq's curves exhibit quite high variability when resampled at PANALESIS reconstruction intervals. This is evident in Figures 5 and 6, where the variability in estimates underscores the inherent challenges in reconstructing past sea levels. These observations highlight the importance of understanding and constraining uncertainties in palaeogeographic models.

Despite the differences observed when comparing our sea-level curves with Haq's curves, our uncertainties are well understood and constrained. For instance, we recognize that sea-level changes are highly sensitive to the global ocean basin size, which directly affects the volume. An error margin of just 1% in the basin size can result in a sea-level difference of more than 35 meters.

Additionally, our modeled topography is significantly influenced by the ages of geological features. This sensitivity is evident in the different scenarios (Table 2), where a ± 50% variation in feature ages can lead to a sea-level uncertainty of up to 120 meters. Understanding these sensitivities allows us to better constrain our models and improve their accuracy.

Despite these sensitivities, our dual-control model ensures that reconstructions are dynamically coherent and grounded in geological data. This approach allows us to produce fully quantified maps that are validated against sea-level curves derived from a completely different methodology, namely sequential stratigraphy. This validation underscores the robustness of our model and the reliability of our reconstructions.

5. Conclusion

This study highlights issues related to the reproducibility crisis (Baker, 2016). Here, we have not been able to exactly reproduce previous results (Vérard et al., 2015) because the UNIL model is not available anymore, and because, although having similarities, the PANALESIS v0 has been developed from scratch. Despite heavy efforts put into the re-operationalization of the processing code, this case thus underlines the problem of reproducibility due to (i) changes in the programming language and supporting software, (ii) necessary methods divergences and (iii) a lack of proper data management and archiving procedures.

Our results show that new sea-level evolution curves created using the `TopoChronia` plugin for QGIS follow similar trends as previously published results, despite punctual important differences.

These differences are explained by (i) methodological differences such as a change in the reference oceanic volume value, the interpolation method, or how the added water load is corrected and (ii) untracked modifications in the input model since the initial results were published.

For what concerns PANALESIS v1, we observe strong agreement with data from the literature which show sea-level values following the same trend and in the range of uncertainties due to short term processes such as melting, or formation, of continental ice.

These new palaeogeographic maps will set the ground for climate simulation and allow better understanding the dynamics of ice sheets formation, strongly controlled by the presence of land masses at the poles.

Disclaimer

The authors declare that there is no conflict of interest, financial or otherwise, regarding the publication of this paper.

Acknowledgements

We acknowledge financial support from the Swiss National Science Foundation (SNSF) under Sinergia grant #213539: *Long-term evolution of the Earth from the base of the mantle to the top of the atmosphere: Understanding the mechanisms leading to 'greenhouse' and 'icehouse' regimes*.

References

Allen, P. A., Allen, J. R., 2005. *Basin Analysis: Principles and Applications 2nd Edition*. Blackwell Publishing, Incorporated, Oxford OX4 1JF, United Kingdom.

Aminov, J., Dupont-Nivet, G., Ruiz, D., Gailleton, B., 2023. Paleogeographic Reconstructions Using QGIS: Introducing Terra Antiqua Plugin and Its Application to 30 and 50 Ma Maps. *Earth-Science Reviews*, 240, 104401.

Baker, M., 2016. 1,500 Scientists Lift the Lid on Reproducibility. *Nature*, 533(7604), 452–454.

Barker, M., Chue Hong, N. P., Katz, D. S., Lamprecht, A.-L., Martinez-Ortiz, C., Psomopoulos, F., Harrow, J., Castro, L. J., Gruenpeter, M., Martinez, P. A., Honeyman, T., 2022. Introducing the FAIR Principles for Research Software. *Scientific Data*, 9(1), 622.

Charette, M., Smith, W., 2010. The Volume of Earth's Ocean. *Oceanography*, 23(2), 112–114.

Fretwell, P., Pritchard, H. D., Vaughan, D. G., Bamber, J. L., Barrand, N. E., Bell, R., Bianchi, C., Bingham, R. G., Blankenship, D. D., Casassa, G., Catania, G., Callens, D., Conway, H., Cook, A. J., Corr, H. F. J., Damaske, D., Damm, V., Ferraccioli, F., Forsberg, R., Fujita, S., Gim, Y., Gogineni, P., Griggs, J. A., Hindmarsh, R. C. A., Holmlund, P., Holt, J. W., Jacobel, R. W., Jenkins, A., Jokat, W., Jordan, T., King, E. C., Kohler, J., Krabill, W., Riger-Kusk, M., Langley, K. A., Leitchenkov, G., Leuschen, C., Luyendyk, B. P., Matsuoka, K., Mouginot, J., Nitsche, F. O., Nogi, Y., Nost, O. A., Popov, S. V., Rignot, E., Rippin, D. M., Rivera, A., Roberts, J., Ross, N., Siegert, M. J., Smith, A. M., Steinhage, D., Studinger, M., Sun, B., Tinto, B. K., Welch, B. C., Wilson, D., Young, D. A., Xiangbin, C., Zirizzotti, A., 2013. Bedmap2: Improved Ice Bed, Surface and Thickness Datasets for Antarctica. *The Cryosphere*, 7(1), 375–393.

Goddéris, Y., Donnadieu, Y., Le Hir, G., Lefebvre, V., Nardin, E., 2014. The Role of Palaeogeography in the Phanerozoic History of Atmospheric CO2 and Climate. *Earth-Science Reviews*, 128, 122–138.

Gregory, J. M., Huybrechts, P., Raper, S. C. B., 2004. Threatened Loss of the Greenland Ice-Sheet. *Nature*, 428(6983), 616–616.

Hallam, A., Cohen, J. M., 1997. The Case for Sea-Level Change as a Dominant Causal Factor in Mass Extinction of Marine Invertebrates. *Philosophical Transactions of the Royal Society of London. B, Biological Sciences*, 325(1228), 437–455.

Haq, B., 2018. Triassic Eustatic Variations Reexamined. *GSA Today*, 28(12), 4–9.

Haq, B., Al-Qahtani, 2005. Phanerozoic Cycles of Sea-Level Change on the Arabian Platform. *GeoArabia*, 10(2), 127–160.

Haq, B., Schutter, S. R., 2008. A Chronology of Paleozoic Sea-Level Changes. *Science*, 322(5898), 64–68.

Haq, B. U., Hardenbol, J., Vail, P. R., 1987. Chronology of Fluctuating Sea Levels Since the Triassic. *Science*, 235(4793), 1156–1167.

Hardenbol, JAN., Thierry, J., Farley, M., Jacquin, T., Graciansky, P., Vail, P., 1998. Mesozoic and Cenozoic Sequence Stratigraphy of Europen Basins. *SEPM Spec. Publ.*, 60, SEPM Society for Sedimentary Geology, 3–29.

Isacks, B., Oliver, J., Sykes, L. R., 1968. Seismology and the New Global Tectonics. *Journal of Geophysical Research (1896-1977)*, 73(18), 5855–5899.

Le Pichon, X., 1968. Sea-Floor Spreading and Continental Drift. *Journal of Geophysical Research (1896-1977)*, 73(12), 3661–3697.

Lunt, D. J., Farnsworth, A., Loptson, C., Foster, G. L., Markwick, P., O'Brien, C. L., Pancost, R. D., Robinson, S. A., Wrobel, N., 2016. Palaeogeographic Controls on Climate and Proxy Interpretation. *Climate of the Past*, 12(5), 1181–1198.

Marcilly, C. M., Torsvik, T. H., Conrad, C. P., 2022. Global Phanerozoic Sea Levels from Paleogeographic Flooding Maps. *Gondwana Research*, 110, 128–142.

McKenzie, D. P., Parker, R. L., 1967. The North Pacific: An Example of Tectonics on a Sphere. *Nature*, 216(5122), 1276–1280.

Miall, A. D., 1996. *The Geology of Fluvial Deposits*. Springer, Berlin, Heidelberg.

Miller, K. G., Kominz, M. A., Browning, J. V., Wright, J. D., Mountain, G. S., Katz, M. E., Sugarman, P. J., Cramer, B. S., Christie-Blick, N., Pekar, S. F., 2005. The Phanerozoic Record of Global Sea-Level Change. *Science*, 310(5752), 1293–1298.

Morgan, W. J., 1968. Rises, Trenches, Great Faults, and Crustal Blocks. *Journal of Geophysical Research (1896-1977)*, 73(6), 1959–1982.

NOAA, 2022. NOAA National Centers for Environmental Information. 2022: ETOPO 2022 15 Arc-Second Global Relief Model.

Payton, C., 1977. *Seismic Stratigraphy: Application to Hydrocarbon Exploration*. American Association of Petroleum Geologists.

QGIS Development Team, 2025. QGIS geographic information system. QGIS Association.

Scotese, C., 2021. An Atlas of Phanerozoic Paleogeographic Maps: The Seas Come In and the Seas Go Out. *Annual Review of Earth and Planetary Sciences*, 49(Volume 49, 2021), 679–728.

Snedden, J. W., Liu, C., 2010. A Compilation of Phanerozoic Sea-Level Change, Coastal Onlaps and Recommended Sequence Designations; #40594 (2010). *Search and Discovery Article 40594, AAPG.*

Stampfli, G. M., Borel, G. D., 2002. A Plate Tectonic Model for the Paleozoic and Mesozoic Constrained by Dynamic Plate Boundaries and Restored Synthetic Oceanic Isochrons. *Earth and Planetary Science Letters*, 196(1), 17–33.

Stampfli, G. M., Hochard, C., Vérard, C., Wilhem, C., von-Raumer, J., 2013. The Formation of Pangea. *Tectonophysics*, 593, 1–19.

Stein, C. A., Stein, S., 1992. A Model for the Global Variation in Oceanic Depth and Heat Flow with Lithospheric Age. *Nature*, 359(6391), 123–129.

Vail, P., Audemard, F., Bowman, S., Eisner, P., Perez-Cruz, C., 1991. The Stratigraphic Signatures of Tectonics, Eustasy and Sedimentology — an Overview. G. Einsele, W. Ricken, A. Seilacher (eds), *Cycles and Events in Stratigraphy*, Springer-Verlag, Berlin, 617–659.

Vail, P. R., Mitchum, Jr., R. M., Thompson, III, S., 1977. Seismic Stratigraphy and Global Changes of Sea Level, Part 4: Global Cycles of Relative Changes of Sea Level. C. E. Payton (ed.), *Seismic Stratigraphy — Applications to Hydrocarbon Exploration*, 26, American Association of Petroleum Geologists, 0.

Vérard, C., 2017. Statistics of the Earth's Topography. *OALib*, 04(06), 1–50.

Vérard, C., 2019. Panalesis: Towards Global Synthetic Palaeogeographies Using Integration and Coupling of Manifold Models. *Geological Magazine*, 156(2), 320–330.

Vérard, C., 2021. 888–444 Ma Global Plate Tectonic Reconstruction With Emphasis on the Formation of Gondwana. *Frontiers in Earth Science*, 9.

Vérard, C., 2022. On the Reliability of the Panalesis (V.0) Palæogeographic Maps. *SSRN Electronic Journal*.

Vérard, C., 2024. On Greenhouse and Icehouse Climate Regimes over the Phanerozoic. *Terra Nova*, 36(4), 292–297.

Vérard, C., Hochard, C., Baumgartner, P. O., Stampfli, G. M., Liu, M., 2015. 3D Palaeogeographic Reconstructions of the Phanerozoic versus Sea-Level and Sr-ratio Variations. *Journal of Palaeogeography*, 4(1), 64–84.

Vine, F., Hess, H. H., 1968. Sea floor spreading. A. Maxwell (ed.), *The Sea*, 4, Princeton University Press, Princeton, NJ.

Wilgus, C., Hastings, B., Kendall, C., Posamentier, H., Ross, C., Van Wagoner, J., 1988. *Sea Level Changes: An Integrated Approach*. 43, SEPM Spec. Pub.

Wilkinson, M. D., Dumontier, M., Aalbersberg, I. J., Appleton, G., Axton, M., Baak, A., Blomberg, N., Boiten, J.-W., da Silva Santos, L. B., Bourne, P. E., Bouwman, J., Brookes, A. J., Clark, T., Crosas, M., Dillo, I., Dumon, O., Edmunds, S., Evelo, C. T., Finkers, R., Gonzalez-Beltran, A., Gray, A. J. G., Groth, P., Goble, C., Grethe, J. S., Heringa, J., 't Hoen, P. A. C., Hooft, R., Kuhn, T., Kok, R., Kok, J., Lusher, S. J., Martone, M. E., Mons, A., Packer, A. L., Persson, B., Rocca-Serra, P., Roos, M., van Schaik, R., Sansone, S.-A., Schultes, E., Sengstag, T., Slater, T., Strawn, G., Swertz, M. A., Thompson, M., van der Lei, J., van Mulligen, E., Velterop, J., Waagmeester, A., Wittenburg, P., Wolstencroft, K., Zhao, J., Mons, B., 2016. The FAIR Guiding Principles for Scientific Data Management and Stewardship. *Scientific Data*, 3(1), 160018.

Wright, N. M., Seton, M., Williams, S. E., Whittaker, J. M., Müller, R. D., 2020. Sea-Level Fluctuations Driven by Changes in Global Ocean Basin Volume Following Supercontinent Break-Up. *Earth-Science Reviews*, 208, 103293.

Zonn, I. S., Kostianoy, A. G., Semenov, A. V., Joksimović, A., Đurović, M., 2021. Mediterranean Sea. I. S. Zonn, A. G. Kostianoy, A. V. Semenov, A. Joksimović, M. Đurović (eds), *The Adriatic Sea Encyclopedia*, Springer International Publishing, Cham, 226–228.